COVER SHEET FOR TECHNICAL MEMORANDUM

TITLE—AAP Electrical Power System Capabilities   TM- 70-1022-6
in the Earth Resources Mission Mode

DATE— March 23, 1970

FILING CASE NO(S)— 620

AUTHOR(S)—   W. W. Hough
B. W. Moss
J. J. Sakolosky

FILING SUBJECT(S)
(ASSIGNED BY AUTHOR(S))—   Apollo Applications Program
Electrical Power Systems
Earth Resources Experiments

ABSTRACT

During periods of earth resources experimentation, the
AAP Cluster attitude will be controlled such that the fixed ex-
periment axis is continuously aligned with the local vertical.
In this attitude mode, solar array power output is substantially
less than power generated in the usual solar inertial attitude
when the arrays are continuously pointed at the sun. The fact
that the angle of incidence of the sun's rays is other than
zero causes a cosine loss in incident energy plus an increase
in the energy reflected from the solar cell coverslides. The
attitude is such that a larger average percentage of the arrays
powering the Airlock system will be shadowed by the ATM arrays.
On the positive side, the average temperature of the arrays will
be lower than in the solar inertial mode, and therefore the
electrical power output will be higher for a given incident
solar flux.

The basic assumptions made for this analysis are that
the experiment viewing axis is directly opposite the solar array
outward normal, and that this axis is aligned with the local
vertical at an orbital midnight and remains aligned until a
subsequent midnight.   In order to perform earth resources
experimentation for one to several consecutive orbits, the
system power requirements must be reduced, and/or an operational
ground rule that the state-of-charge of each battery must
return to 100% during the illuminated portion of each orbit
must be set aside. It appears that an acceptable combination
of decreased power requirements and permissible battery depth-
of-discharge can be chosen such that two, and maybe three
consecutive orbits are possible without imposing any severe
restrictions on the sun-line/orbit-plane angle, β. Further, if
the earth resources targets of interest are all north of 25°
latitude (i.e. the U.S.A.), then the power capability can be
substantially improved by locating the experiment axes 20-30
degrees away from their assumed location on the plus-Z Cluster
axis toward the minus-Y axis.

Pages – 39
Code – 2C
BCR – 110089

CATEGORY 03

BA-145A (8-68)

DISTRIBUTION

COMPLETE MEMORANDUM TO

CORRESPONDENCE FILES:

OFFICIAL FILE COPY
plus one white copy for each
additional case referenced

TECHNICAL LIBRARY (4)

NASA Headquarters

H. Cohen/MLR
J. H. Disher/MLD
W. B. Evans/MLO
L. K. Fero/MLV
J. P. Field, Jr./MLP
W. H. Hamby/MLO
T. E. Hanes/MLA
T. A. Keegan/MA-2
M. Savage/MLT
W. C. Schneider/ML

Goddard Space Flight Center

J. T. Skladany/713

Langley Research Center

P. R. Kurzhals/AMPD

MSC

R. G. Brown/ES-16
C. N. Crews/KS
W. R. Cunningham/CB
R. E. Durkee/ES-5
R. L. Frost/KS
O. K. Garriott/CB
F. C. Littleton/KM
R. M. Machell/KF
P. S. Miglicco/KS
O. G. Smith/KF
H. E. Whitacre/KM

MSFC

R. M. Aden/S&E-ASTR-E
W. B. Chubb/S&E-ASTR-SGD
J. C. Cody/S&E-ASTN-PLA

COMPLETE MEMORANDUM TO

MSFC (continued)

D. N. Counter/S&E-ASTR-MA
C. B. Graff/S&E-ASTR-EP
G. B. Hardy/PM-AA-EI
G. D. Hopson/S&E-ASTN-PL
E. H. Hyde/S&E-ASTN-PF
H. F. Kennel/S&E-ASTR-A
G. F. McDonough/S&E-CSE-A
E. F. Noel/S&E-ASTR-SI
W. C. Patterson/S&E-ASTN-PLA
J. W. Sims/s&E-ASTN-PTA
J. D. Stroud/S&E-ASTR-SE
J. W. Thomas/PM-AA
H. F. Trucks/S&E-ASTN-PTA
J. L. Vaniman/S&E-ASTN-PT
R. D. Wegrich/S&E-CSE-AA
A. P. Woosley/S&E-ASTR-SEC
H. E. Worley/S&E-AERO-DOI

Martin-Marietta

H. S. Nassen/Denver
E. F. Bjoro/Washington
M. S. Imamura/Denver
R. W. Wilson/Denver

McDonnell-Douglas

G. Weber/Eastern Division

Bellcomm

A. P. Boysen
D. R. Hagner
W. G. Heffron
B. T. Howard
J. Z. Menard
J. M. Nervik
I. M. Ross
P. F. Sennewald
J. W. Timko
R. L. Wagner
M. P. Wilson
Departments 2031, 2034 Supervision
Department 1024 File
Division 102
Central Files

BELLCOMM, INC.
955 L'ENFANT PLAZA NORTH, S.W.   WASHINGTON, D.C. 20024

SUBJECT: AAP Electrical Power System
Capabilities in the Earth Resources
Mission Mode - Case 620

DATE: March 23, 1970

FROM: W. W. Hough
B. W. Moss
J. J. Sakolosky

TM-70-1022-6

TECHNICAL MEMORANDUM

I. INTRODUCTION

Electrical power for Apollo Applications Program spacecraft is generated by solar cell arrays. There are two solar array/battery systems; the AM system is mounted on the Workshop and Airlock Module and the ATM system is mounted on the Apollo Telescope Mount. When illuminated, the solar arrays convert incident solar energy into electrical energy. Some of this energy is used to power system loads and the rest is stored in batteries. Spacecraft power is supplied by these batteries when the array is not illuminated. Although they are the same in principal, the two systems are different in design and possess different operating characteristics. Although it is now planned to operate the systems in parallel for power sharing under nominal conditions, the systems have been treated separately in the past and that practice will be continued in this paper.

In the nominal AAP attitude mode, which is known as solar inertial, the vehicle is stabilized so that the arrays are pointed directly at the sun throughout the entire sunlit portion of the orbit, thus the per-orbit energy output of the arrays is maximized. Several earth-resources experiments have been proposed for AAP which, when operating, require a different attitude mode. In the earth-resources mission mode, the viewing axes of the spacecraft-fixed experiments must be continually aligned with the local vertical to within some small angular tolerance. These experiments will, in the main, perform observations of the sunlit earth and will therefore be fixed to the vehicle on the side opposite the active face of the arrays. The array energy output will therefore be reduced, but not eliminated.

The objective of the work reported in this paper has been to accurately determine the capabilities of the two AAP electrical power systems in the earth-resources mission mode.

Taking as a base the current AAP Cluster configuration as shown in Figure 1, system capabilities further depend on:

a)   the attitude profile,

b)   the sun-line/orbit plane angle, β,

c)   the position of the experiment viewing axis relative to the solar arrays,

d)   the time into the mission that the experiments are performed,

and e)   the maximum permissible depth of discharge of the batteries.

With all of the above specified, the number of consecutive experiment passes that are possible from the power standpoint can be determined if we also specify:

f)   the estimated average power requirements on both systems independent of the experiments

and g)   the power source for the experiments themselves (AM or ATM) and their power requirement.

II.   ATTITUDE PROFILE

In Reference 1, three possible attitude profiles are discussed which meet the stated requirements of the earth resources experiments. They are alike in that all position the experiment viewing axes along the local vertical when the target (sub-spacecraft point) is properly illuminated by the sun, and in that the vehicle X-axis (roll axis) is kept in the orbital plane parallel to the velocity vector. They differ in how this attitude is acquired, starting from the solar inertial attitude.

It is shown in Reference 1 that to minimize the expense of attitude maneuvers while maximizing experiment opportunities in sunlight, an attitude profile known as midnight acquisition must be used. This profile begins with a vehicle roll maneuver between orbital sunset and orbital midnight to place the experiment viewing axis in the orbital plane such that the experiments will look directly down at midnight. At midnight, the orbital rate is induced about the normal to the orbital plane. The experiment axis then remains along the local vertical for some integral number of midnight-to-midnight orbits. After the last experimental pass, the opposite of the acquisition sequence is carried out; the orbital rate is removed at midnight and the vehicle is rolled back to solar inertial before orbital sunrise.

OWS SOLAR ARRAY PANELS

INSTRUMENT UNIT

ORBITAL WORKSHOP

LOWER PAYLOAD SHROUD

AIRLOCK MODULE

MULTIPLE DOCKING ADAPTER

COMMAND MODULE

SERVICE MODULE

ATM SOLAR ARRAY PANELS

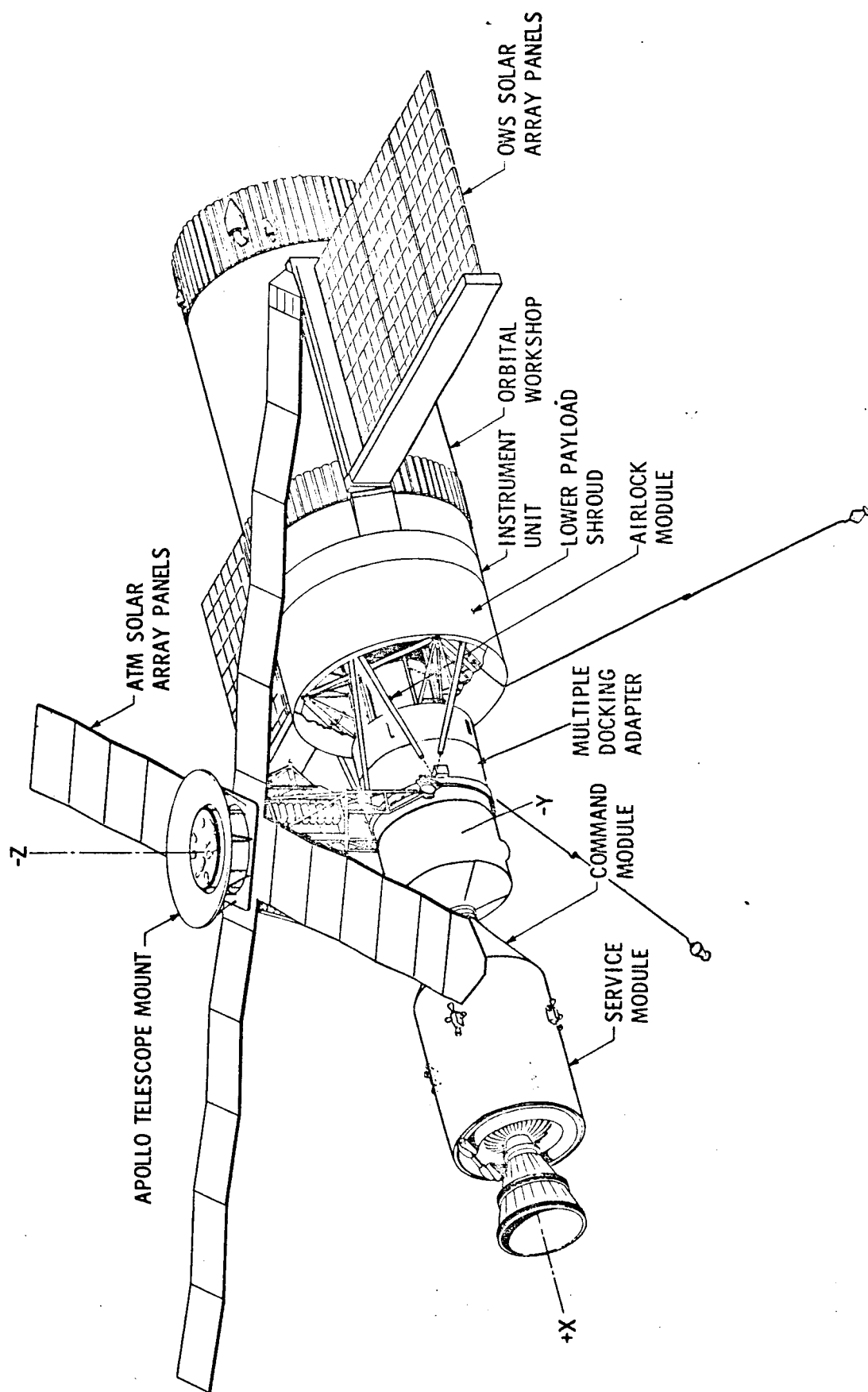APOLLO TELESCOPE MOUNT

-Z

-Y

+X

FIGURE 1 - AAP CLUSTER

The midnight acquisition profile has been adopted for this study. In the Baseline Reference Mission document (Ref. 2) the specification of the orientation of the Cluster in the solar inertial mode is such that the plus-X axis (CSM end) is in the direction of the velocity vector at orbital noon. The CSM will therefore lag at midnight, and the minus-X (OWS end) will be in the direction of the velocity vector throughout the earth resources mission mode. If either of the other two acquisition modes, noon acquisition or local target acquisition, discussed in Reference 1 are used, then the opposite is the case - the leading end in the earth resources mode will be the CSM end.

III. EXPERIMENT POSITION

The outward normals to the solar arrays of the AAP Cluster are all in the direction of the minus-Z Cluster axis. In the prior wet Workshop configuration, which was to use a different attitude profile and had movable solar arrays, the viewing axis of the multiband photography experiment was optimally located along the Cluster plus-Z axis. This experiment position has remained for all proposed earth resources experiments in the dry Workshop configuration. From electrical power and thermal control standpoints, the plus-Z experiment position is not necessarily the optimum in the attitude mode just described. The optimum depends on the range of target latitudes, the accessibility to these targets, and the direction of flight.

In this study, the plus-Z experiment position was adopted. In a later section optimal, or at least more favorable, positioning will be discussed.

IV. INSTANTANEOUS SOLAR ARRAY POWER OUTPUT

The instantaneous solar array power output in the earth resources mission mode, P_{SA}, can be evaluated by the following equation:

$$P_{SA} = \cos \lambda \cdot P_N(T) \cdot (1-L_R) \cdot (1-L_D) \cdot (1-L_S) \tag{1}$$

Each term of (1) is discussed in detail in the following paragraphs.

cos λ:

      λ is the angle of solar incidence; that is the angle between the vector to the sun and the outward normal to the solar array, which is the minus-Z Cluster axis. The incident solar power per unit area of the array is directly proportional to the cosine of λ. With the experiments along the plus-Z, the solar array normal will be coincident with the local vertical. In this attitude the cosine of λ is the product of the cosines of the minimum angle between the sun vector and the orbit plane, β, and the orbit position angle, η.

$$\cos \lambda = \cos \beta \cos \eta \qquad (2)$$

These two angles are defined in Reference 3 and shown in Figure 2. β is positive if the sub-orbital-noon point is south of the sub-solar point.* (β as shown is negative.) η measures the angular position in the orbit of the spacecraft relative to orbital noon, and is positive (as shown) in the direction of the orbital velocity vector. Both β and η are time varying, and neither vary linearly. β varies due to the earth's rotation about the sun and orbital regression. Figure 3 is the time history of β for a mission launched at 3:00 p.m. EST on July 15 to a 235 NM, 50° inclination orbit. The limits on β are plus and minus the sum of the orbital inclination and the angle between the ecliptic and equatorial planes; for a 50° inclination, $-73°27' \leq \beta \leq +73°27'$. A pass of the satellite from one orbital noon to the next is equivalent to a 360° increase in η. The time rate of change of η is not constant, again because of orbital regression and the earth's rotation about the sun. In Appendix A, however, an expression for the <u>average</u> noon-to-noon satellite period, $T_{S\ AVG}$, is derived, and that period has been used in this study in a linear approximation of the relation between η and time.

$$\dot{\eta} \approx 2\pi/T_{S\ AVG} \qquad \text{rad/hr} \qquad (3)$$

      With the assumed location of the experiment viewing axes along the Cluster plus-Z axis, the effect of β on power system capabilities is independent of the sign of β in the case of the ATM, and almost independent in the case of the AM. The slight dependency of the AM capabilities on the sign of β is due to nonsymmetric shadowing of the AM arrays, which is in turn

---

    *This definition of positive β is consistent with the definition contained in the Baseline Reference Mission (Ref. 2), but opposite to the definition of Reference 3.
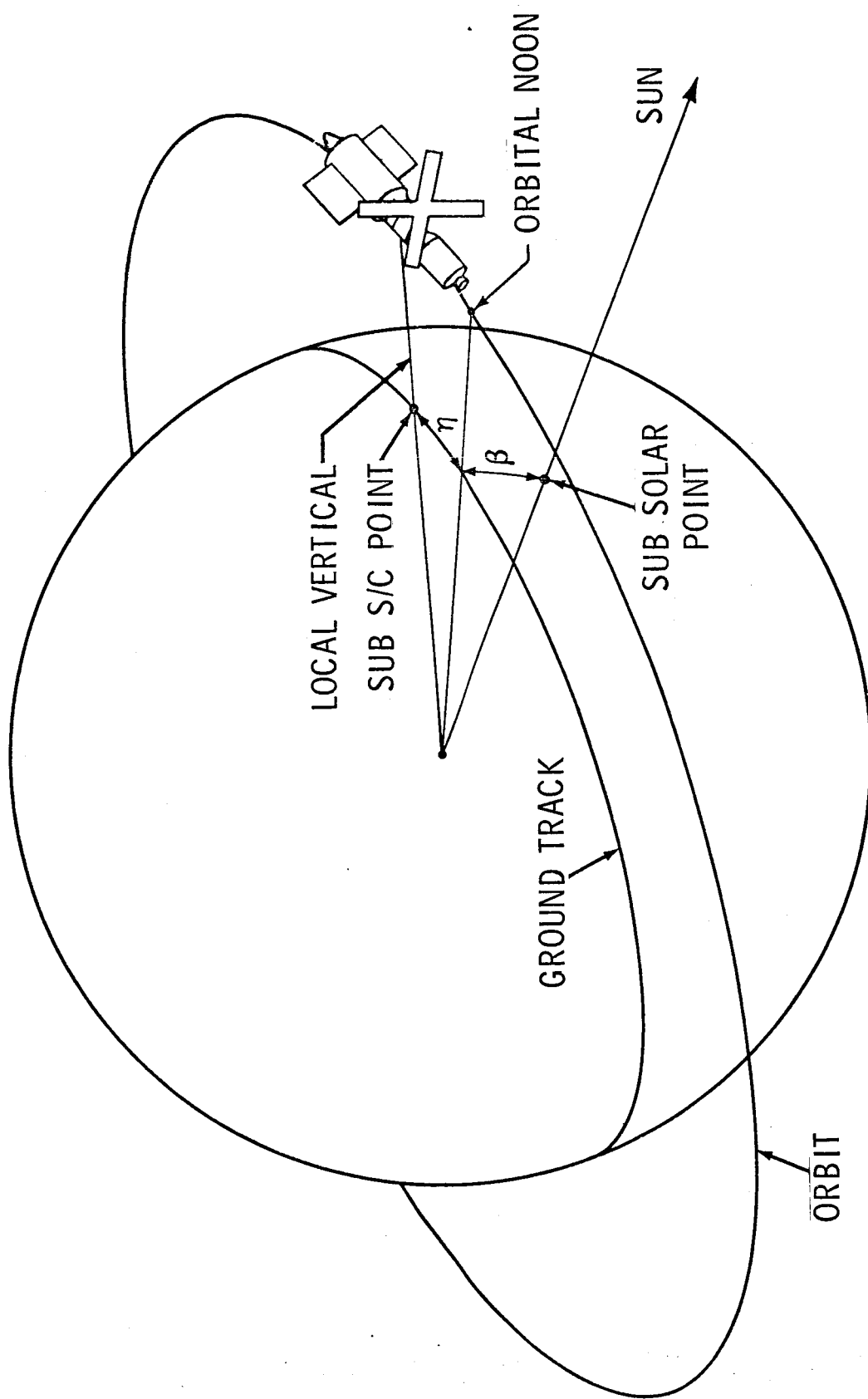
LOCAL VERTICAL

SUB S/C POINT

ORBITAL NOON

SUN

η

β

SUB SOLAR POINT

GROUND TRACK

ORBIT

FIGURE 2 - ORBITAL GEOMETRY

ORBITAL INCLINATION = 50°
LAUNCH DATE = JULY 15
LAUNCH TIME = 3:00 PM EST
ALTITUDE = 235 NM

UPPER LIMIT ON β FOR
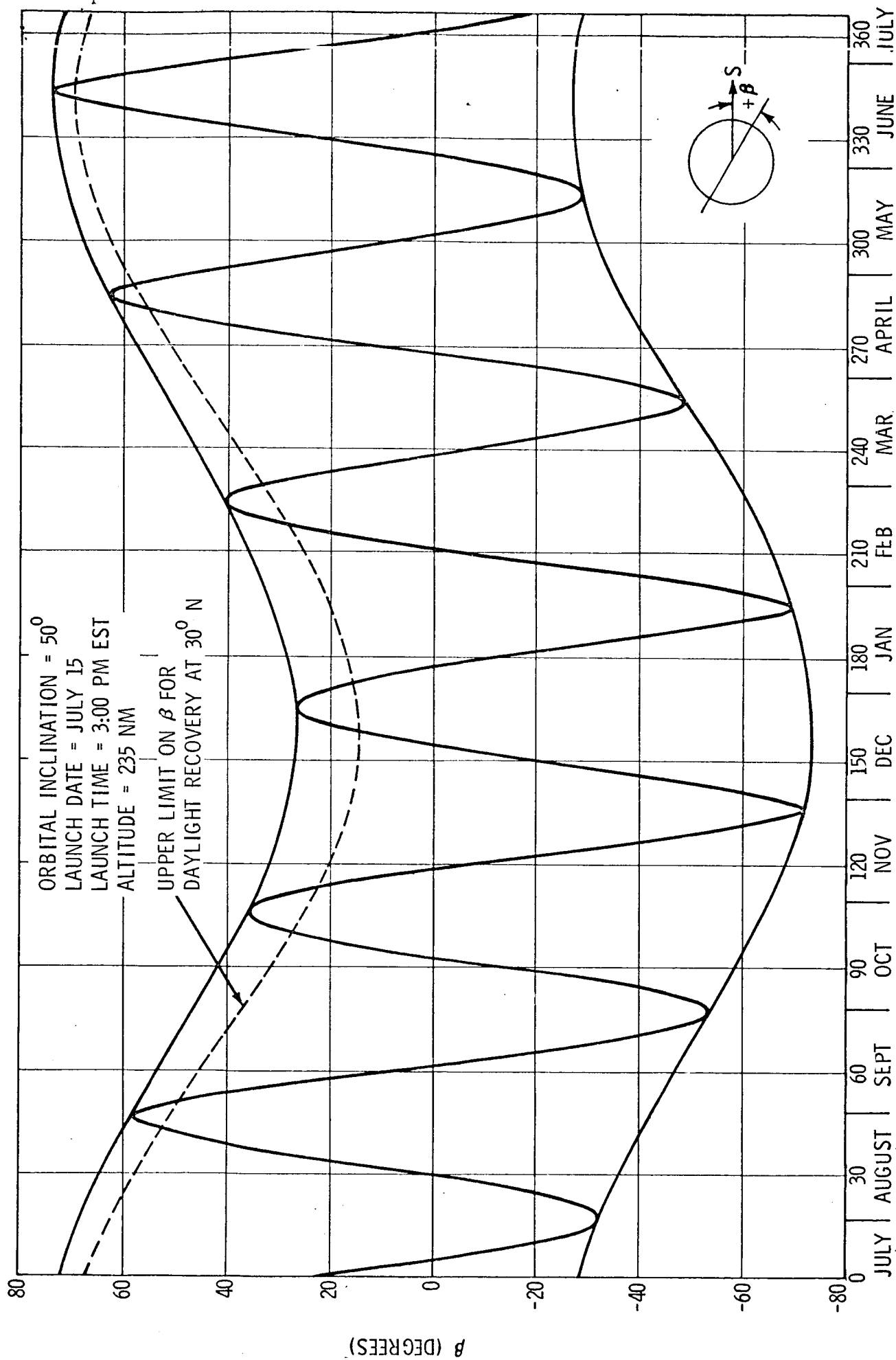DAYLIGHT RECOVERY AT 30° N

FIGURE 3 - BETA HISTORY

due to the offset of the arrays. However, the difference is
undiscernable in plots of AM capabilities vs β. Therefore only
positive values of β are used in plots of capabilities, with
the understanding that the results apply equally well for negative
β of the same absolute values.

It can be seen from equation (2) that cos λ will be
negative whenever cos η is negative as cos β is always positive.
However, P_{SA} in equation (1) can never be negative, but will be
zero when cos η is zero or negative. In other words, the array
will not see the sun and will not produce power when η is between
90° and 270° in the earth resources mission mode. Therefore, we
need consider solar array output only when η is between -90° and
+90°.

$P_N(T)$:

$P_N(T)$ is the temperature dependent power output of
the full array at normal solar incidence, air mass zero, and
beginning of life. Solar arrays converting incident radiant
energy into electrical energy are predictably affected by the
temperature of the array which is itself affected by the incident
radiant energy. It is well-known that the open-circuit voltage
is an inverse function of temperature and is essentially
unaffected by incident intensity while short-circuit current is
a linear function of incident intensity and is essentially un-
affected by temperature. The maximum power of an array at any
given intensity, then, is an inverse function of temperature.
Various sources give maximum power temperature coefficients
ranging from -0.42% per °C to -0.485% per °C. (-0.234% per °F
to -0.27% per °F.)

The two solar array systems in AAP both use identical
solar cells arranged as modules to provide the desired power
levels at the desired voltage levels. The cells are 2 cm × 2 cm
N on P silicon cells with a nominal base resistivity of 10 ohm-cm
and an active area of 3.8 cm^2. The conversion efficiency is
taken as 10 per cent. From this, the nominal power output of
each cell with incident normal solar power of 140 mw/cm^2 can be
determined.

$$P_{cell} = 140 \times 3.8 \times 0.10 = 53.2 \text{ mw/cell}$$

The AM array consists of 240 modules of 1136 cells each for a total of 272640 cells and the ATM array consists of 360 modules of 684 cells each for a total of 246240 cells. So,

$$P_{AM} = 53.2 \times 10^{-3} \times 272640 = 14504 \text{ w}$$

$$P_{ATM} = 53.2 \times 10^{-3} \times 246240 = 13100 \text{ w}$$

These nominal total array outputs are based on the cells being at a temperature of 30°C (86°F) and do not include losses for assembly into an array. The losses are summarized in the following table

	AM	ATM
Coverslides and adhesive	2.0%	2.0%
Cell mismatch	3.0	3.0
Diode loss (0.8v)	1.4	2.0
Line loss (1.0v)	1.75	2.5
Total loss	8.15%	9.5%

The array power capabilities at 86°F are therefore

$$P_{AM} = 14504 \ (1-0.0815) = 13322 \text{ w}$$

$$P_{ATM} = 13100 \ (1-0.095) = 11855 \text{ w}$$

Taking the temperature coefficient as -0.465% per °C, or -.258% per °F, we can write the expressions for $P_N(T)$. For the AM system:

$$P_N(T) = 13322 \ (1-.00258 \ (T-86)) \qquad (4-a)$$

and for the ATM system:

$$P_N(T) = 11855 \ (1-.00258 \ (T-86)) \qquad (4\text{-}b)$$

where T is the temperature of the array in degrees F.

When these expressions are evaluated at the rated operating temperatures of the two systems, the results are in agreement with the MSFC published rated power capabilities to within 0.14%.

T:

To make use of the expressions for $P_N(T)$ just developed, an analysis of the array temperature profile is required. Several analyses of array temperature profiles for different attitude profiles have been performed by J. W. Powers, including the earth resources mission mode under consideration here. His work is reported in Reference 4. He modeled the array as a single two surface node with the appropriate absorptivity and emissivity on each face, and assumed these properties were identical for the two arrays. The array planar surfaces receive time varying direct solar, earth reflected solar, and earth emitted IR thermal fluxes as functions of altitude (taken as the baseline 235 NM circular orbit), attitude, and position angles relative to the sun, β and η. The incident flux profile together with the array physical properties were used to determine the array temperature profile. Power's results for the earth resources mission mode are shown in Figure 4 for the pertinent range of η and for four β angles.

The curves of Figure 4 can be duplicated to within a few percent with a fairly simple curve-fit equation, which was developed to ease computational effort within the computer program that predicts instantaneous solar array power output. Further, interpolation for different β angles is unnecessary. This expression is

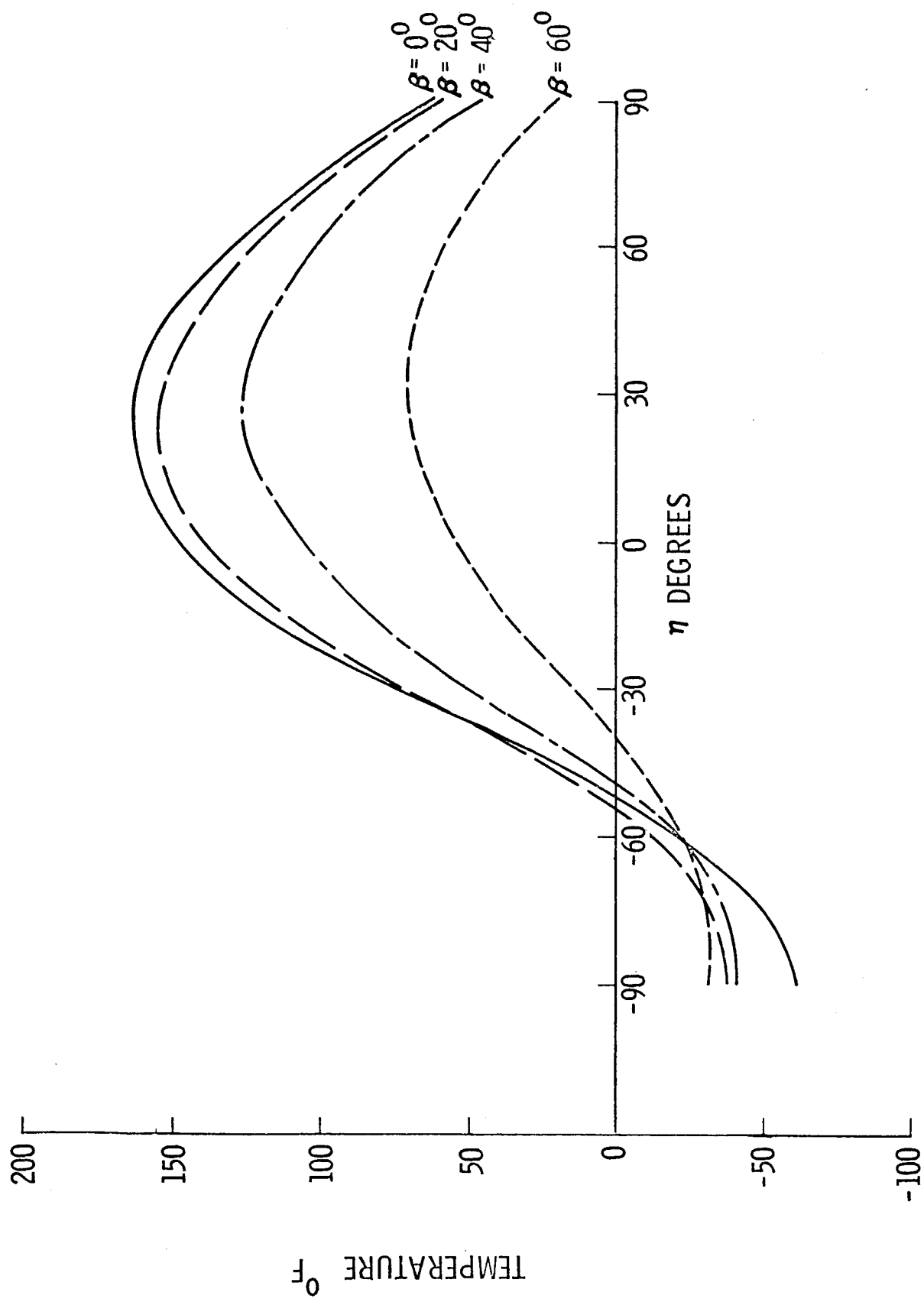$$T = A + B \sin \left(180° \cdot \frac{n+35-C}{125-C}\right) + D \qquad (5)$$

FIGURE 4 – SOLAR ARRAY TEMPERATURE VS. ORBITAL POSITION

where

$$A = 59 - .00088846 \ \beta^{2.617}$$

$$B = 104 - .02144 \ \beta^{1.907}$$

$$C = .00022212 \ \beta^{2.617}$$

$$D = \begin{cases} E + F, & \eta \leq + 15° \\ 0, & \eta > + 15° \end{cases}$$

where

$$E = -.09808 \ (60-\beta)^{1.081}$$

$$F = 0.14517 \ (60-\beta)^{1.107} \ \sin \left(180° \cdot \frac{\eta+40}{70}\right)$$

When using these equations, η must be maintained in the range of $-90° \leq + \eta \leq + 90°$ (use of 280° rather than -80° will give an erroneous result), and β must be positive. Both must be input in degrees. The temperature, T, will be in degrees F.

$1-L_R$:

Because of reflection of incident light off the solar cell coverslide and because of transmission loss within the coverslide, the intensity of light reaching the surface of the cell is decreased from that reaching the coverslide. The transmission loss is assumed to be a constant 2%. The reflective loss is a function of the angle of incidence and the index of refraction of the coverslide material. In Reference 5, the following expression was developed for determination of the magnitude of the reflective loss:

$$\text{Percent loss} = 100\% \cdot \frac{\sin^2(\lambda-\chi)}{\sin^2(\lambda+\chi)} \left[1 + \frac{\cos^2(\lambda+\chi)}{\cos^2(\lambda-\chi)} \right] \qquad (6)$$

where λ is the angle of incidence and χ is the angle of refraction. λ and χ are related to the index of refraction of the coverslide material by Snell's law:

$$\frac{\sin \lambda}{\sin \chi} = \text{index of refraction}$$

For the fused silica coverslides used in AAP, the index of refraction averages 1.47 over the wave lengths of interest.

At normal incidence, equation (6) reduces through small angle approximations to

$$\begin{matrix}\text{Percent loss at} \\ \text{normal incidence}\end{matrix} = 100\% \cdot \frac{(\text{index of refraction} -1)^2}{(\text{index of refraction} +1)^2} \qquad (7)$$

which, when evaluated, gives a 3.63% loss. Applying this loss to (4a) and (4b) gives rated solar array power outputs at normal incidence that would be lower than the MSFC published capabilities by approximately the amount of the loss. Presumably, therefore, the loss due to reflection at normal incidence is already included in (4a) and (4b) through the assumed conversion efficiency of 10%. This presumption is supported by the fact that 10 ohm-cm N on P silicon cells characteristically have a conversion efficiency of approximately 10.5%. In this study, therefore, the degraded transmittance of the coverslide due to reflection at the cover-slide-space interface has been normalized to 100% at normal incidence. The normalized transmittance, 1-reflective loss $(1-L_R)$, in percent is

$$100\% \ (1-L_R) = \frac{100\% - \text{percent loss by (6)}}{100\% - \text{percent loss at normal incidence by (7)}} \qquad (8)$$

The normalized transmittance is plotted in Figure 5 vs the angle of incidence.

$1-L_D$:

The solar-to-electrical power conversion efficiency of solar cells degrades due to environmental radiation. The purpose of the coverslides is to minimize this degradation, but they do not eliminate it. The time dependent degradation used in AAP has been legislated at 1/2% per month. The term L_D in equation
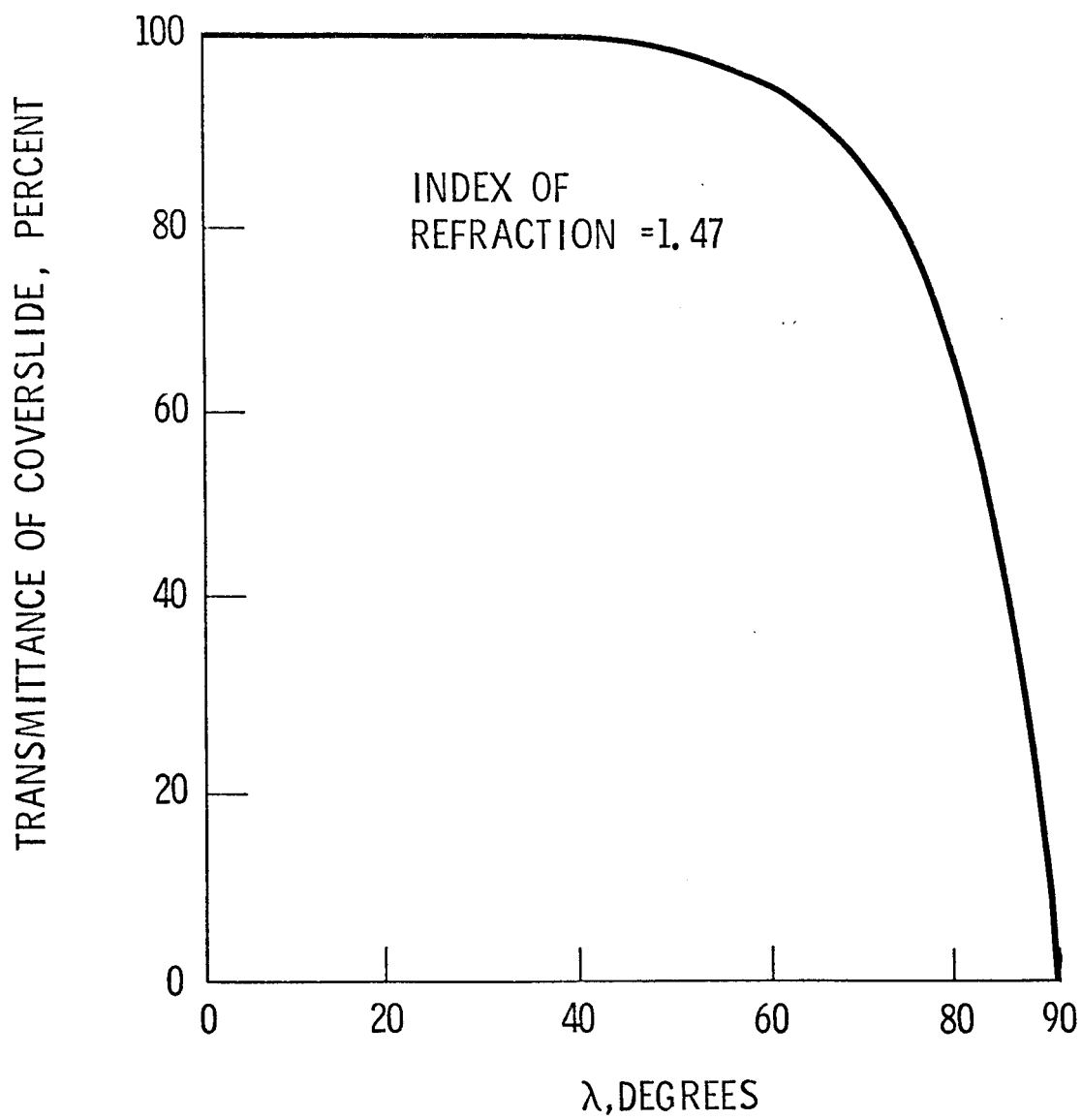
FIGURE 5 - PERCENT INCIDENT LIGHT TRANSMITTED THROUGH COVERSLIDE
(NORMALIZED TO 100% AT NORMAL INCIDENCE)

(1) is therefore simply 0.005 d where d is the time into the mission in months.

$$1-L_D = 1 - 0.005\ d \tag{9}$$

$1-L_S$:

This term accounts for the degradation in power output of the AM solar arrays due to shading by the ATM array.

$$L_S = \frac{\text{Shaded Area of Solar Array}}{\text{Total Area of Solar Array}} \tag{10}$$

L_S is equal to zero when calculating power at the ATM array since this array is never shaded during the portion of the orbit where cos λ is positive.

Shading of the AM arrays by the ATM array is a function of the sun angle, β, and the orbital position angle, η. A computer program (documented in Reference 6) which calculates shading of the AM arrays has been used to obtain the data required for this study. This program is used as a subroutine in the more general computer program used to calculate instantaneous power produced by the solar arrays.

Figure 6A illustrates the ratio of unshaded area to the total area (i.e., $1-L_S$) of the AM solar arrays as a function of η for β angles of 0°, 20°, 40°, and 60°. Figure 6B shows the same ratio for β angles of 0°, -20°, -40°, and -60°. The sign of β makes a difference because of the difference in the Z location of the two AM panels (see Figure 1). These data apply for the midnight acquisition attitude profile where the CSM is the lagging vehicle and shading occurs in the later part of the sunlit portion of the orbit, roughly between η angles of -5° and +80° for medium and small sun angles. For large β angles (β > 50°), the portion of the orbit during which shading occurs is considerably less.

If an attitude profile is used that results in the opposite vehicle orientation, that is with the CSM the leading vehicle, the array shadowing will occur in the opposite half of the orbit. Shadowing data for this case can be taken directly from Figures 6 by reversing the signs on the η scale and the β angle.
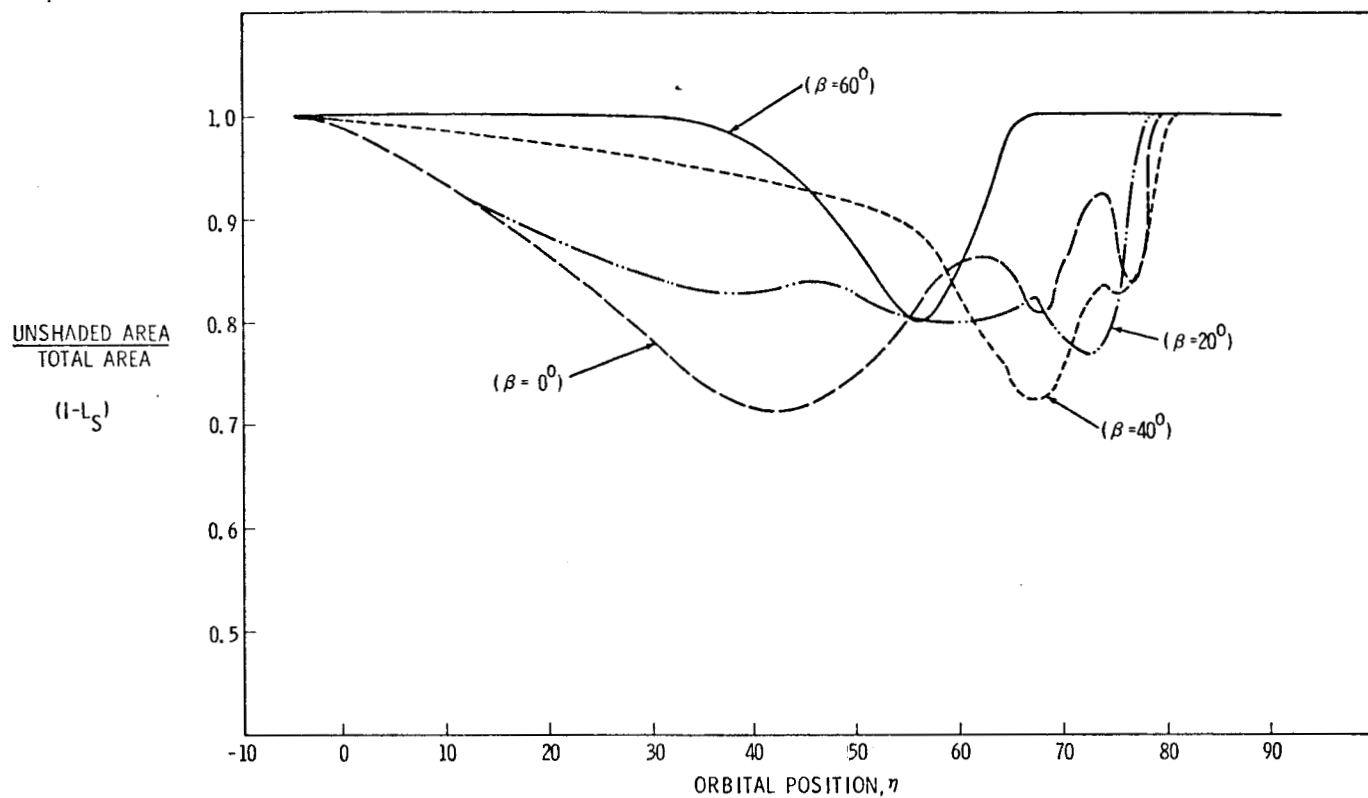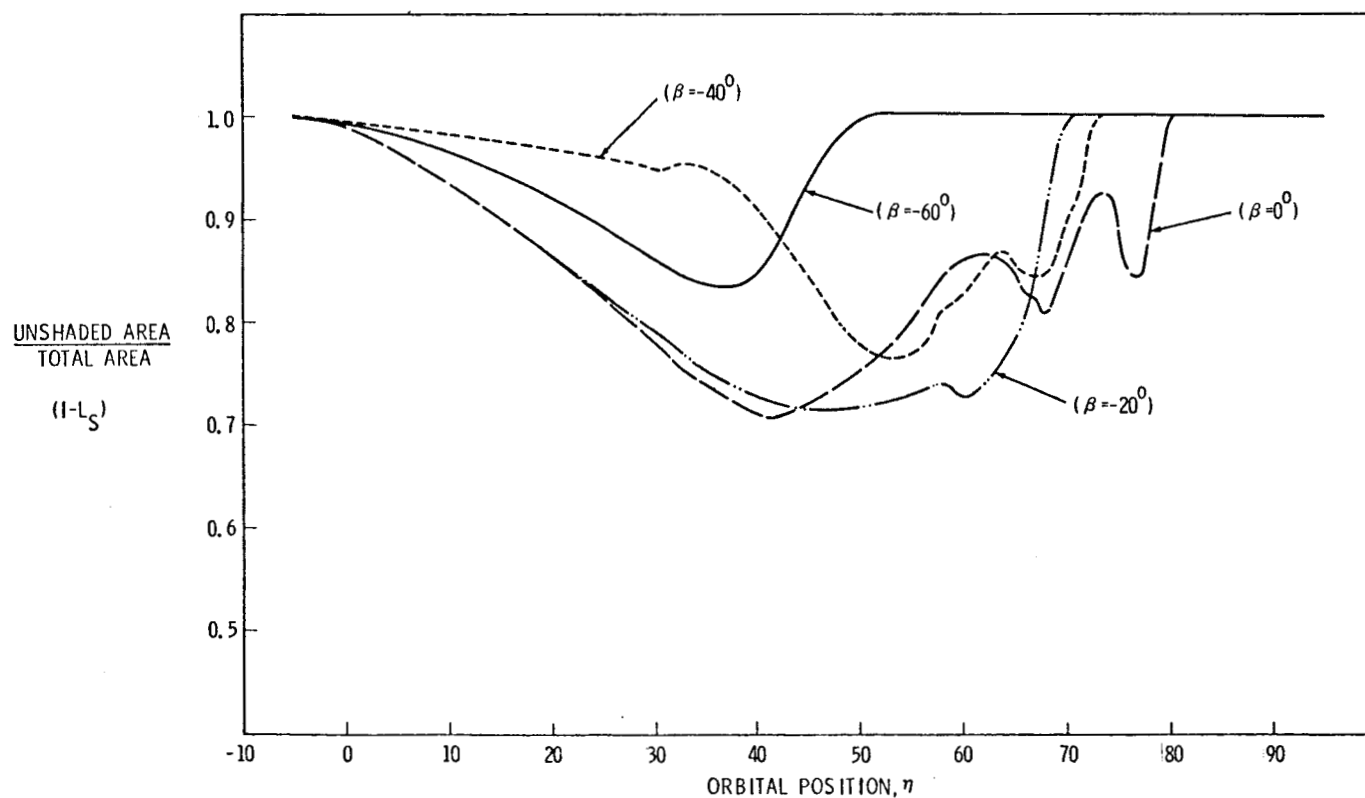
FIGURE 6A - SUN ANGLES GREATER THAN OR EQUAL TO ZERO

FIGURE 6B - SUN ANGLES LESS THAN OR EQUAL TO ZERO

FIGURE 6 - RATIO OF UNSHADED AREA TO TOTAL AREA OF AM SOLAR ARRAYS AS
A FUNCTION OF SUN ANGLE AND ORBITAL POSITION.

Notice from Figure 6 that there is no readily predictable or consistent pattern that the shaded area follows as a function of β angle. This results from the geometry of the situation. The cruciform pattern of the ATM solar array causes a sequential shading of the AM panels as the Cluster changes its orbital position. The unequal displacements of the two AM panels from the plane of the ATM array also add to the effect of non-symmetric shading patterns. As can be seen from Figure 6, worst case shading occurs for small β angles. The maximum shading of the AM arrays occurs for orbital position angles between 40° and 50°. At this point in the orbit, approximately 30% of the total area of the AM arrays is shaded.

V.   SOLAR ARRAY ENERGY OUTPUT

The energy output of the solar array between the time t_1 and the time t_2 is simply the integral of (1) over the time increment

$$W_{SA} = \int_{t_1}^{t_2} P_{SA} \, dt \tag{11}$$

Since time and orbit position angle, η, are related approximately by a constant given by (3),

$$\eta = \int \dot{\eta} \, dt \approx \frac{2\pi}{T_{S_{AVG}}} \, t \tag{12}$$

we can express the energy output of the array as:

$$W_{SA} = \frac{T_{S_{AVG}}}{2\pi} \int_{\eta_1}^{\eta_2} P_{SA} \, d\eta \tag{13}$$

In the earth resources mission mode, the array sees the sun only between orbital 6 a.m. and orbital 6 p.m. The energy output in a single orbit is

$$W_{SA0} = \frac{T_{S_{AVG}}}{2\pi} \int_{-\pi/2}^{\pi/2} P_{SA} \, d\eta \qquad (14)$$

Because of the complexities introduced into P_{SA} by the temperature, time into the mission, coverslide reflection, and array shadowing, (14) must be integrated numerically. A rough approximation for the per-orbit energy output, which is useful in determining trends for different β's or different attitude profiles, can be made by neglecting all terms of (1) except $P_N(T) \cos \lambda$ and treating T as a constant. Then

$$W_{SA0} \approx \frac{T_{S_{AVG}}}{\pi} P_N(T) \cos \beta \qquad (15)$$

The accuracy of the result by (15) depends strongly on the assumed constant temperature, T. With T at 100°F and $\beta=0$, (15) gives a result 4.8% higher than the more accurate ATM energy output predicted by (14).

VI. POWER SYSTEM ENERGY PROFILE

The total electrical energy used (and lost through inefficiencies) during the mission cannot be greater than the total energy output of the solar arrays plus the initial stored energy in the batteries. Further, to insure continuous capability to supply loads, the stored energy must at no time reach zero. The SWS will be launched with all batteries fully charged. Once the solar inertial attitude is acquired, normal operating conditions will permit full recharge of all batteries during the sunlit portion of the orbit, and depth of discharge (DOD) of the batteries during the dark portion of the orbit will not normally be beyond 30%. Higher loads or lower solar array output are occasionally acceptable as long as the stored energy does not vanish. Subsequent to the occurance of such conditions, the batteries must be allowed to recover so the long-term energy balance requirement will be met.

The earth resources mission mode is an example of a condition where the solar array output is substantially below the output in the solar inertial mode. In this attitude, it is unlikely that energy can be balanced on an orbit-to-orbit basis. That is, it is likely that the batteries will not return to 100% state of charge each orbit. In this section, the method for determination of the battery state of charge after some number of orbits in the earth resources mode is given. From this, we can state the capabilities of the power systems during earth resources experimentation.
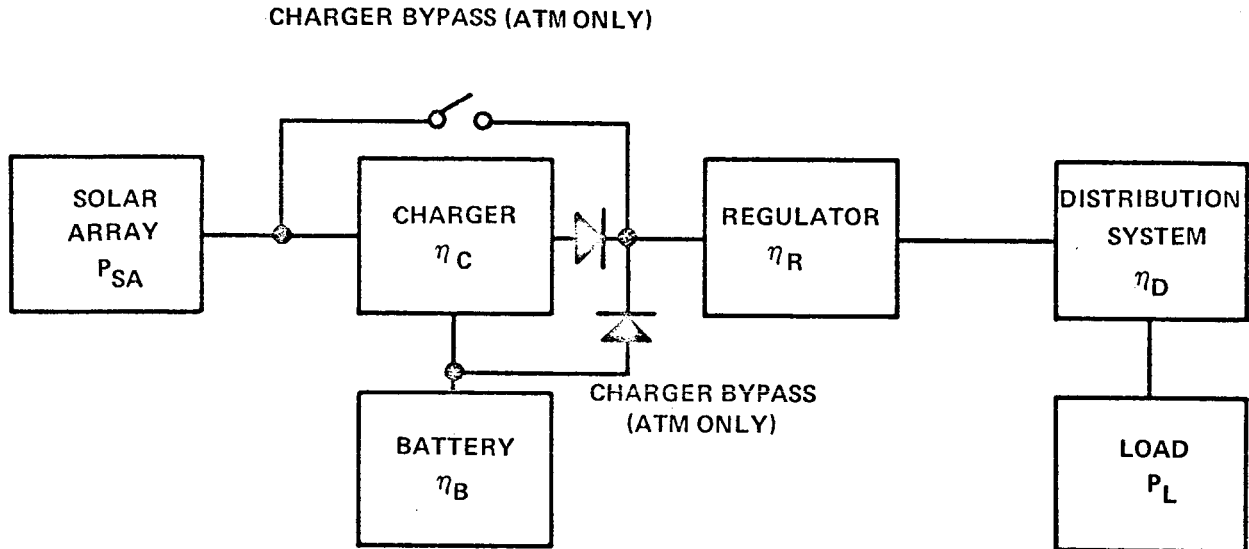
CHARGER BYPASS (ATM ONLY)

FIGURE 7 - SOLAR ARRAY/BATTERY ELECTRICAL POWER SYSTEM

Figure 7 is a simplified schematic of a solar array/ battery power system. P_{SA} is the instantaneous solar array output, and P_L is the instantaneous load on the system. When the load, increased by the power lost in the distribution system and the regulater, is greater than the array output, there is over a time Δt a net loss of energy from the battery.

$$W_{LOSS} = \left(\frac{P_L}{\eta_R \eta_D} - P_{SA} \right) \Delta t \qquad (16)$$

If the array output exceeds the demand, there is a gain in energy in the battery,

$$W_{GAIN} = \eta_C \eta_B \left(P_{SA} - \frac{P_L}{\eta_R \eta_D} \right) \Delta t \qquad (17)$$

where η_C and η_B account for the power lost in the charger and battery. The definitions and values of the efficiencies for the two systems are given in the following table.

		AM	ATM
η_C = charger efficiency		.95	.96
η_B = battery charge utilization or watt hour efficiency		.677	.70
η_D = distribution efficiency		.826	.877
η_R = regulator efficiency		.95	.875

The value of the distribution efficiency for the AM accounts for the fact that power is supplied to the load from either source through the charger. This is not the case in the ATM.

The change in battery state of charge over the time Δt is obtained by dividing the change in energy, given by (16) and (17), by the total energy capacity of the battery system, W_{CAP}. The total capacity of the eight AM batteries is taken as 9108 watt-hours and the eighteen ATM batteries have a total capacity of 9936 watt-hours.

To track the battery state of charge, it is first necessary to determine whether energy is being gained or lost, but this simply entails picking the positive result of (16) or (17). That result is then divided by the capacity and appropriately added to or subtracted from the state-of-charge at the beginning of the period Δt. Continuing this process over time will give a time profile of the battery state of charge. The only restriction is that the state of charge must be within the limits $0 \leq SOC \leq 1$ (i.e.: $0 \leq SOC \leq 100\%$).

In the earth resources mode, the entire state-of-charge profile is not of as much interest as the minimum state of charge that occurs. Specification of a minimum allowable SOC is needed before the capability of the system to support the experiment mode can be stated.

If the system load is constant, or at least repetitive from orbit to orbit, the minimum SOC can be calculated without calculating the entire SOC profile. This can be best explained with the help of Figure 8, which is illustrative of a two-orbit earth resources sequence. On Figure 8, four points are numbered. Point 1 is the point in the orbit where the space-craft, which is in the solar inertial mode, enters earth shadow.

The value of η at point 1, called η_{es} (for earth shadow) in Reference 3, is dependent on β and the altitude of the orbit. It is given by:

$$\eta_{es} = \cos^{-1} \left(-\sqrt{1 - \left[\frac{R}{R+H} \right]^2} \Big/ \cos \beta \right) \qquad (18)$$

where R is the radius of the earth and H is the altitude of the orbit. η_{es} is limited to $90° < \eta_{es} \leq 180°$; if the numerator of the argument of the arc-cosine of (18) is greater than the denominator, η_{es} is to be taken as $180°$, for in this case, the vehicle is constantly in sunlight. For the range of β studied here and the nominal AAP altitude of 235 NM, there will always be earth shadow.
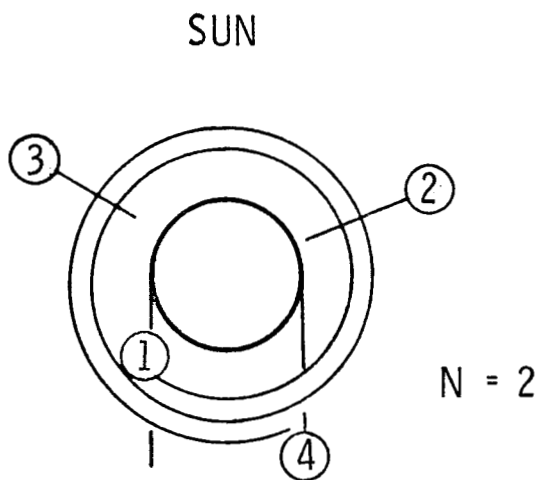
SUN

N = 2

FIGURE 8

Points 2 and 3 are the points where the load, P_L, is exactly equal to the array output times the regulator and distribution efficiencies, $P_{SA}\eta_R\eta_D$.

At point 2, the batteries cease to discharge and begin to charge; at point 3, the opposite occurs. Even with a constant load, points 2 and 3 are not symmetric about $\eta=0$ (noon) because of the non-symmetry in the array temperature profile and, in the case of the AM array, the non-symmetry in shadowing.

Point 4 is the point where the vehicle leaves earth shadow having reacquired the solar inertial attitude, and the arrays abruptly begin delivering more power than the load requires. Neglecting the small change in β over the period in the earth resources mission mode, point 4 and point 1 are symmetric about $\eta=0$.

The segments of the orbit determined by the points just defined are periods when energy is either lost or gained by the batteries. Between points 1 and 2, the energy lost is

$$W_{LOSS\ 1-2} = \int_{1}^{2} \left(\frac{P_L}{\eta_R \eta_D} - P_{SA} \right) dt$$

and the percent decrease in state of charge is

$$\Delta C_{1-2} = 100 \times \frac{W_{LOSS\ 1-2}}{W_{CAP}}$$

The energy gained between 2 and 3 is

$$W_{GAIN\ 2-3} = \int_{2}^{3} \eta_C \eta_B \left(P_{SA} - \frac{P_L}{\eta_R \eta_D} \right) dt$$

and the percent increase in state of charge is

$$\Delta C_{2-3} = 100 \times \frac{W_{GAIN\ 2-3}}{W_{CAP}}$$

We can similarly define ΔC_{3-2} and ΔC_{3-4} as the percent decreases in state of charge between points 3 and 2, and 3 and 4, respectively.

It is assumed that at point 1, the initial state of charge is 100% since the vehicle has just completed a full sunlit pass in the solar inertial attitude. With this initial condition, values for the four ΔC's defined above, and a specified number of orbits (N) in the earth resources mission mode, it is a simple matter to determine the minimum state of charge that the batteries reach. There are, however, several cases that must be examined:

a) If $\Delta C_{2-3} \geq \Delta C_{3-2}$, then the system is operating at or below its continuous power capability. Every orbit the batteries regain their full state of charge. The same minimum occurs every orbit but the first one and is

$$C_{MIN} = 100 - \Delta C_{3-2} \qquad \text{(19-a)}$$

b) If $\Delta C_{1-2} \leq \Delta C_{2-3} < \Delta C_{3-2}$, then the batteries will return to 100% SOC at point 3 after the first experiment pass, but not thereafter. The minimum state of charge might occur at one of two places.

b-1) If $\Delta C_{2-3} > \Delta C_{3-4}$, then the minimum will occur at point 2 just before the last experiment pass and will be

$$C_{MIN} = 100 - (N-1)\, \Delta C_{3-2} + (N-2)\, \Delta C_{2-3} \qquad (19b-1)$$

b-2) If $\Delta C_{2-3} \leq \Delta C_{3-4}$, the minimum will occur at point 4 and will be

$$C_{MIN} = 100 - (N-1)\, (\Delta C_{3-2} - \Delta C_{2-3}) - \Delta C_{3-4} \qquad (19b-2)$$

c) If $\Delta C_{1-2} > \Delta C_{2-3}$, the batteries will not return to 100% SOC at point 3. As in b, we must treat two possible cases.

c-1) If $\Delta C_{2-3} > \Delta C_{3-4}$ the minimum occurs before the last experiment pass

$$C_{MIN} = 100 - \Delta C_{1-2} - (N-1)\, (\Delta C_{3-2} - \Delta C_{2-3}) \qquad (19c-1)$$

c-2) If $\Delta C_{2-3} \leq \Delta C_{3-4}$, the minimum will occur just before the vehicle enters sunlight after the earth resource sequence.

$$C_{MIN} = 100 - \Delta C_{1-2} - (N-1)(\Delta C_{3-2}) + N(\Delta C_{2-3}) - \Delta C_{3-4} \qquad (19c-2)$$

Cases b-2 and c-1 would not have to be included if ΔC_{1-2} and ΔC_{3-4} were exactly equal. The necessary conditions for applicability of these cases could not be satisfied. ΔC_{1-2} and ΔC_{3-4}

would be equal if temperature and shadowing profiles were symmetric about $\eta=0$. Given one set of temperature and shadowing profiles, we can say that it is possible for only one of these cases to occur. We can also say that the range of power requirement over which it will occur is small, because the values of ΔC_{1-2} and ΔC_{3-4} will be close.

VII.   RESULTS

Presentation of power system capabilities for the earth resources mission mode is complicated by the large number of variables that enter the calculations. As the earth resources experiments will be operated only for a short time over the sun-lit earth, it is logical to specify P_L (required to evaluate (16) and (17)) as a profile that peaks when the experiments are on. In this analysis, we have taken the peak as 1070 watts for ten minutes centered about noon, which amounts to an orbital average requirement of 114 watts. In doing so, however, we are forced to specify which system, AM or ATM, is to power the experiments. Both cases have been analyzed. For each case, we are still faced with the problem of displaying the relationship between

- the minimum battery state-of-charge, C_{MIN},

- the power requirement for everything else, P_L,

- the angle β,

- the number of experiment passes, N,

and   - the time into the mission, d .

The last variable listed, d, has the least effect on performance, and we will, for the time being, eliminate it by specifying that it is the beginning of the mission. We will also forget the very small difference in AM power output between cases where β is of the same magnitude but of different sign, which is due to the slightly different shadowing profile. To the accuracy with which the following curves can be plotted and read, the sign of β is immaterial. Then for a given system, a given β, and a choice as to which system powers the experiments, we can present a set of curves like those of Figure 9. These particular curves relate the minimum battery state-of-charge to the average power requirement in the AM system, which includes

the 114 watt average experiment requirement* for one through
five and 10 consecutive experiment passes. For more than one
consecutive pass, the curves all intersect at a power requirement
of approximately 2.1 kw. This is the continuous power capability
at $\beta=0$, beginning of life. Equation (19a) for C_{MIN} applies at
lower power requirements, and (19b-1) applies to approximately
the point where all curves bend downward. This bend occurs when
ΔC_{1-2}, ΔC_{2-3}, and ΔC_{3-4} (see page 23) are all approximately equal.
At higher power levels (19c-2) gives C_{MIN}.

Figures 10 and 11 for the AM are for identical condi-
tions except for β, which is stated on the Figures. Note that
for given minimum state-of-charge and number of passes, the
power capability decreases with increasing β. This suggests
another way to plot the data, namely that of Figure 12. This
plot shows the average power capability vs β and N if the minimum
state of charge is permitted to drop to 40%.

Figure 13 is like the former plots that show minimum
state of charge vs the power requirement, but is for the ATM
system at $\beta=30°$. The power requirement, P_L, used to generate this
data was constant over an orbit; that is, it included no increase
around noon for experiment requirements. It therefore complements
the earlier AM data, which did include the peaks.

The dashed lines on the curves just referenced, at an
AM average power of 2454 watts and an ATM average power of 2022
watts, correspond to estimates of the minimum average power
that might satisfy requirements during the earth resources mission
mode. The AM requirement includes the 114 watt average require-
ment of the experiments. As there is presently much disagreement
and/or uncertainty concerning AAP mission power requirements,
these estimates should be considered as examples of how the
charts can be used to state system capabilities. For instance,
from either Figure 11 or Figure 12, we can state that the AM system
is capable of two consecutive experiment passes at a 2454 watt
average reduced requirement with β up to 60° if the maximum depth
of discharge is permitted to reach 60%.

If the experiments are powered by the ATM rather than
the AM, or if (as now planned) the systems are operated in
parallel, we can state that three consecutive passes are feasible
at the reduced estimated power levels. If the battery depth-of-
discharge is limited to 50%, then β must be below 42°; if 60%

---

*P_L for the AM for this case is the average power requirement
less 114 watts except for the 10 minutes centered about noon, when
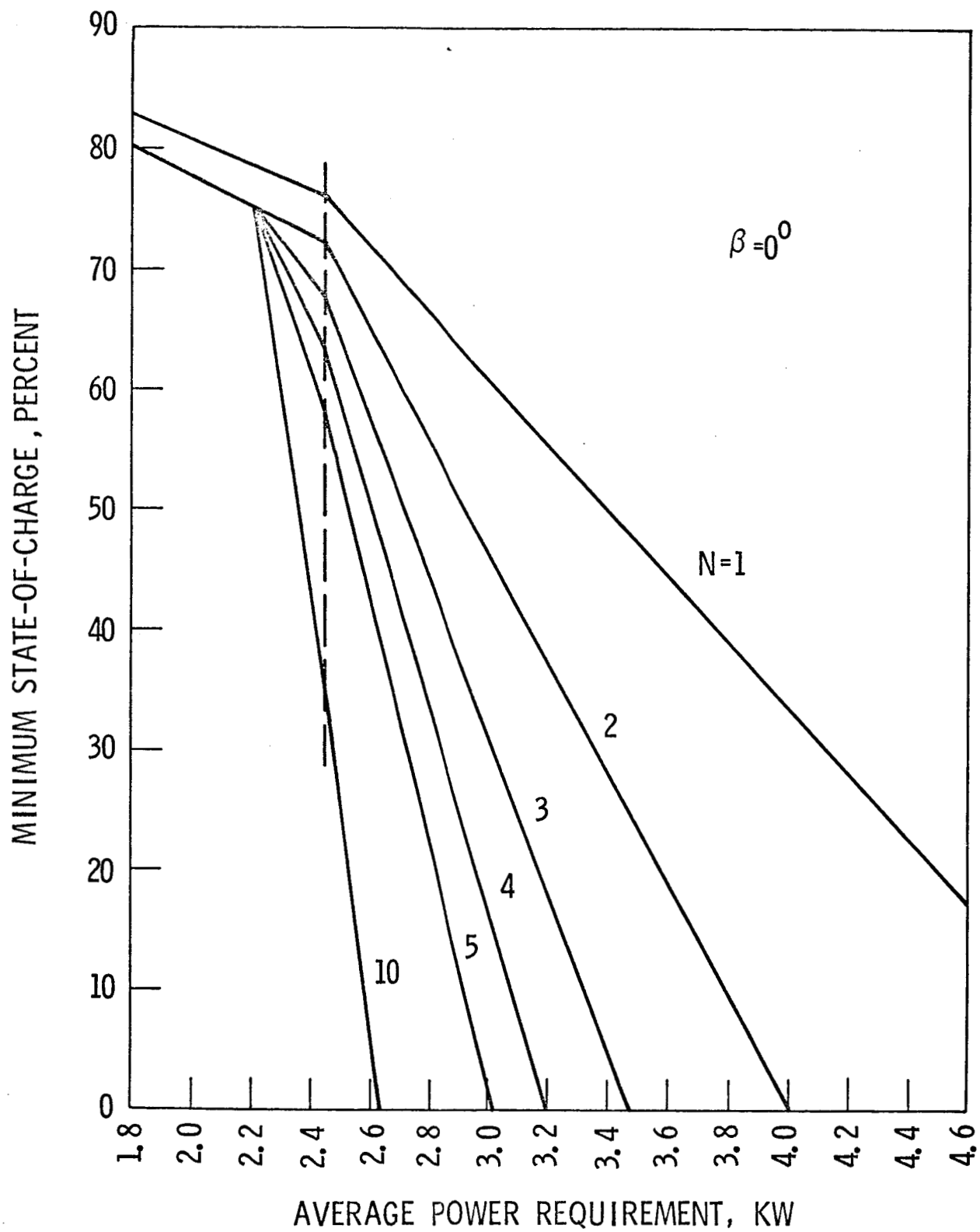it is the average plus 956 watts.

FIGURE 9 - AM BATTERIES — MINIMUM STATE-OF-CHARGE VS. POWER REQUIREMENT DURING N ORBITS IN EARTH POINTING MODE
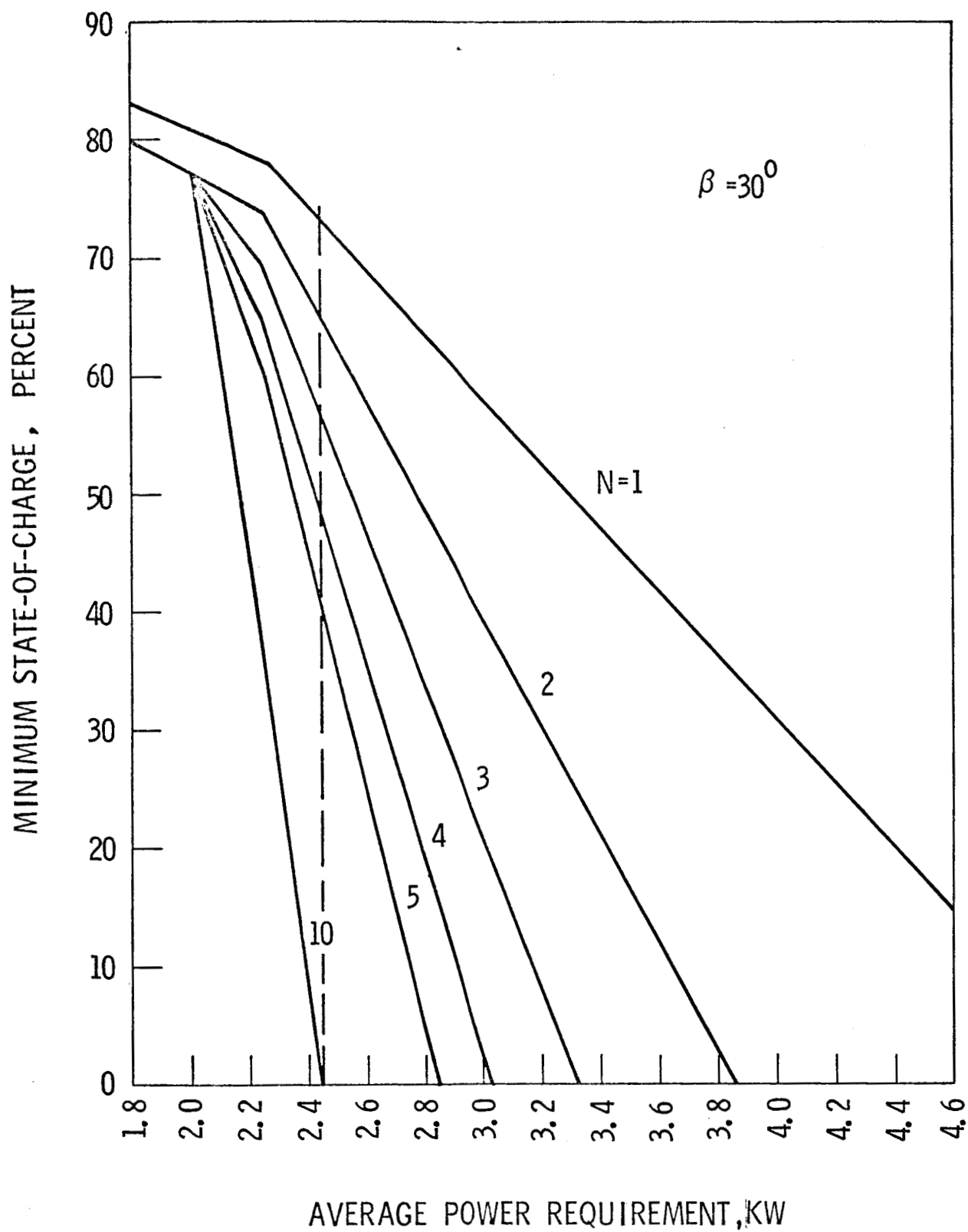
FIGURE 10 - AM BATTERIES — MINIMUM STATE-OF-CHARGE VS. POWER
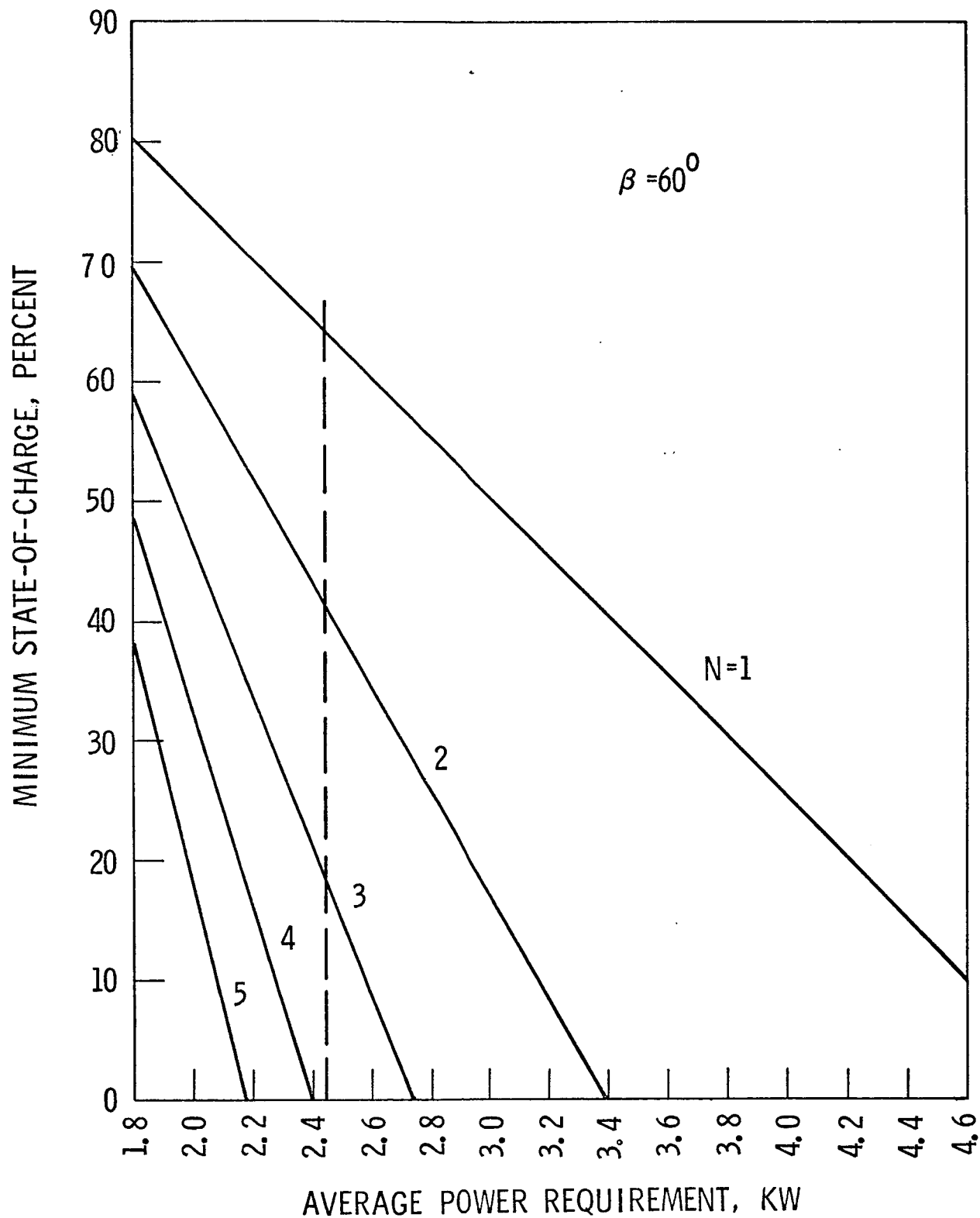REQUIREMENT DURING N ORBITS IN EARTH POINTING MODE

FIGURE 11 - AM BATTERIES — MINIMUM STATE-OF-CHARGE VS. POWER
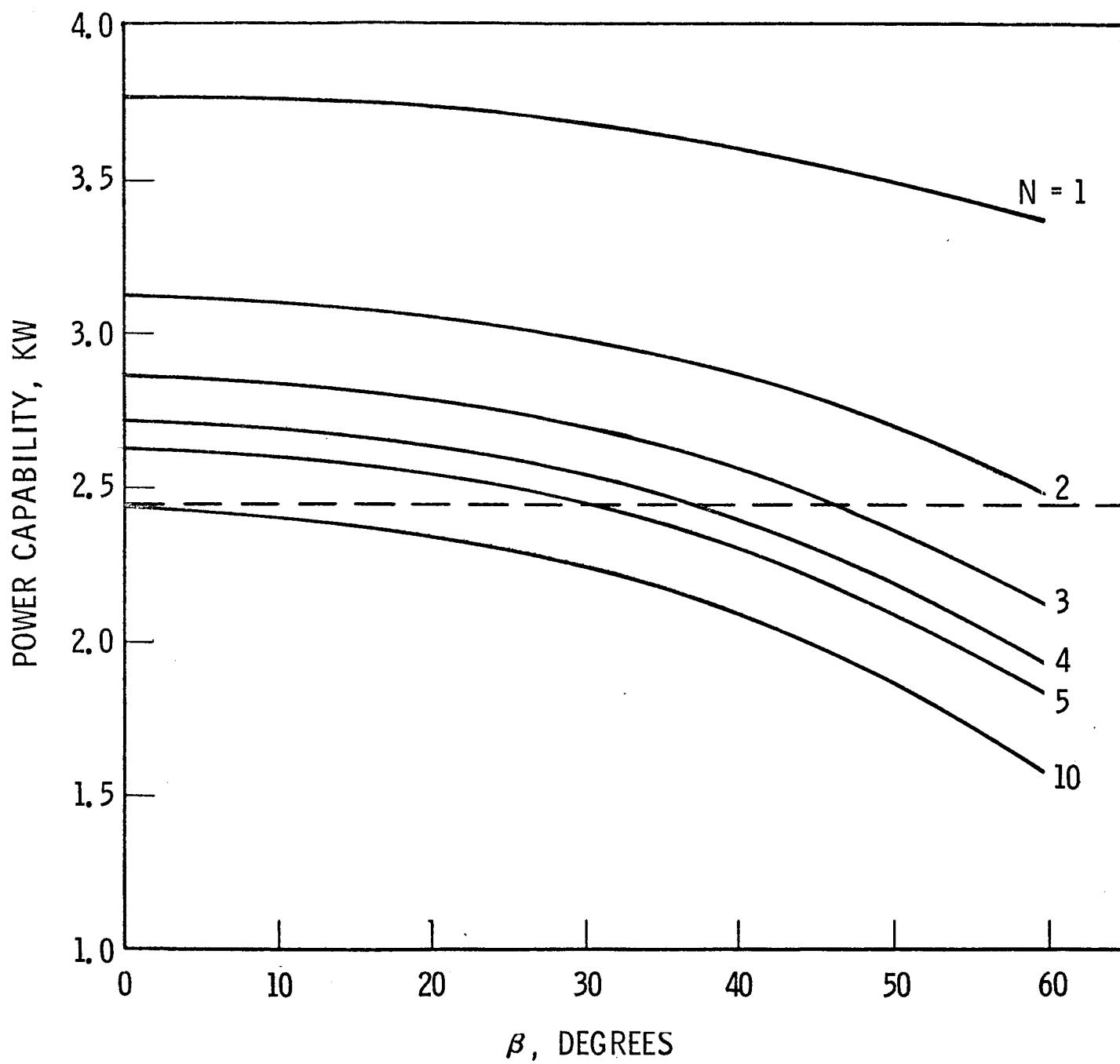REQUIREMENT DURING N ORBITS IN EARTH POINTING MODE

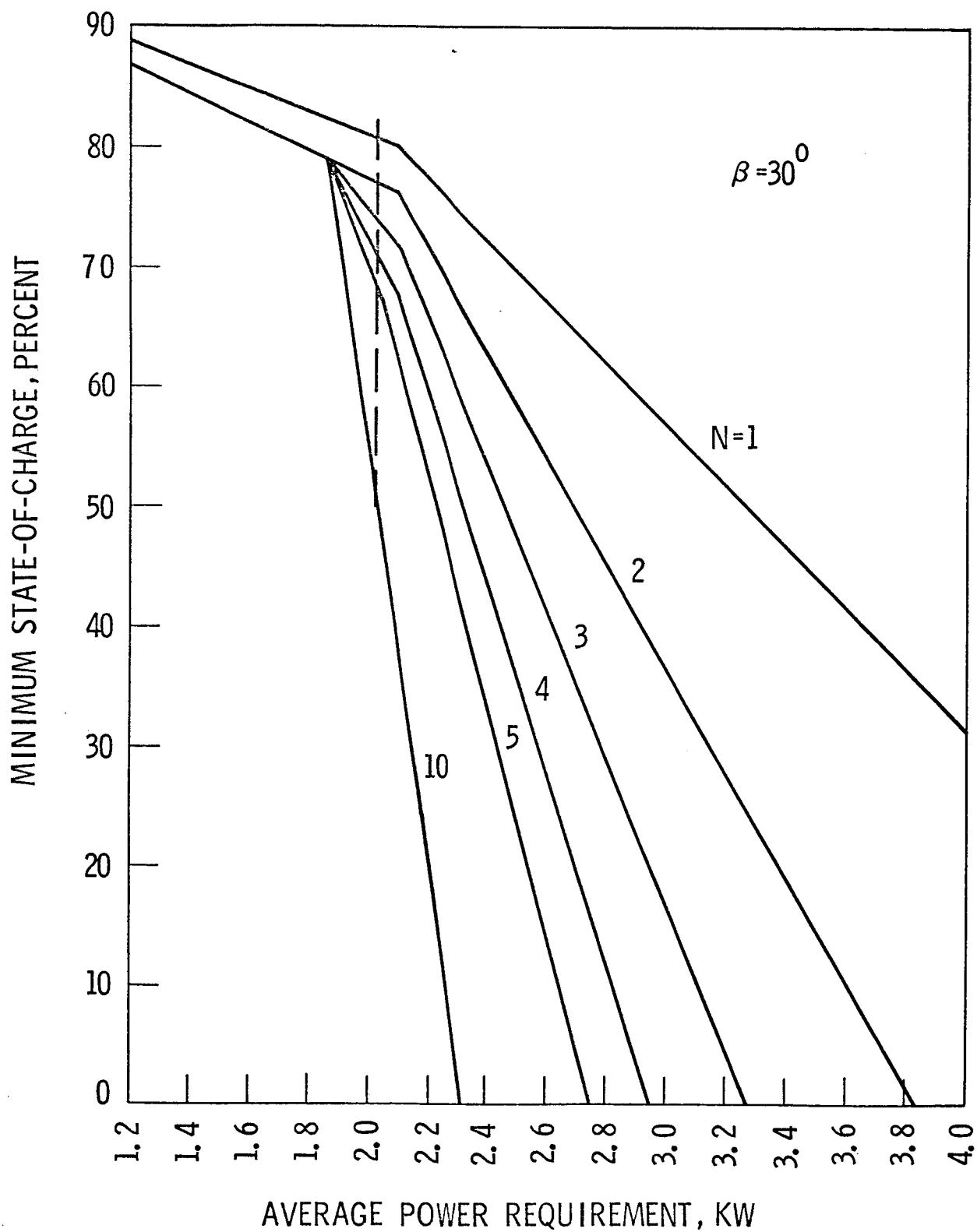FIGURE 12 - AM POWER CAPABILITY WITHOUT EXCEEDING 60% DOD

FIGURE 13 - ATM BATTERIES — MINIMUM STATE-OF-CHARGE VS. POWER
REQUIREMENT DURING N ORBITS IN EARTH POINTING MODE

DOD is permitted, β can be up to 50°, and if three-pass capability over the full range of β (up to 60°) is desired, then the batteries must be permitted to discharge by 70% of their capacity. Such statements are clearly dependent on the assumed power requirement. For a higher power requirement, the capability in terms of number of consecutive orbits or range of β is less.

Let us now look at the effect of lifetime on the power capability. The total life of AAP Workshop I is to be eight months. Figure 14 shows the minimum state-of-charge after three experiment passes vs β at the beginning of life and at the end of life for a 2400 watt load on the AM. We observe that the decrease in the minimum state of charge due to solar cell degradation (difference between curves) is less as the minimum state of charge itself decreases (as β increases). This is logical; as β increases the batteries supply more and the solar arrays supply less of the same total energy, and only the arrays are affected by radiation damage.
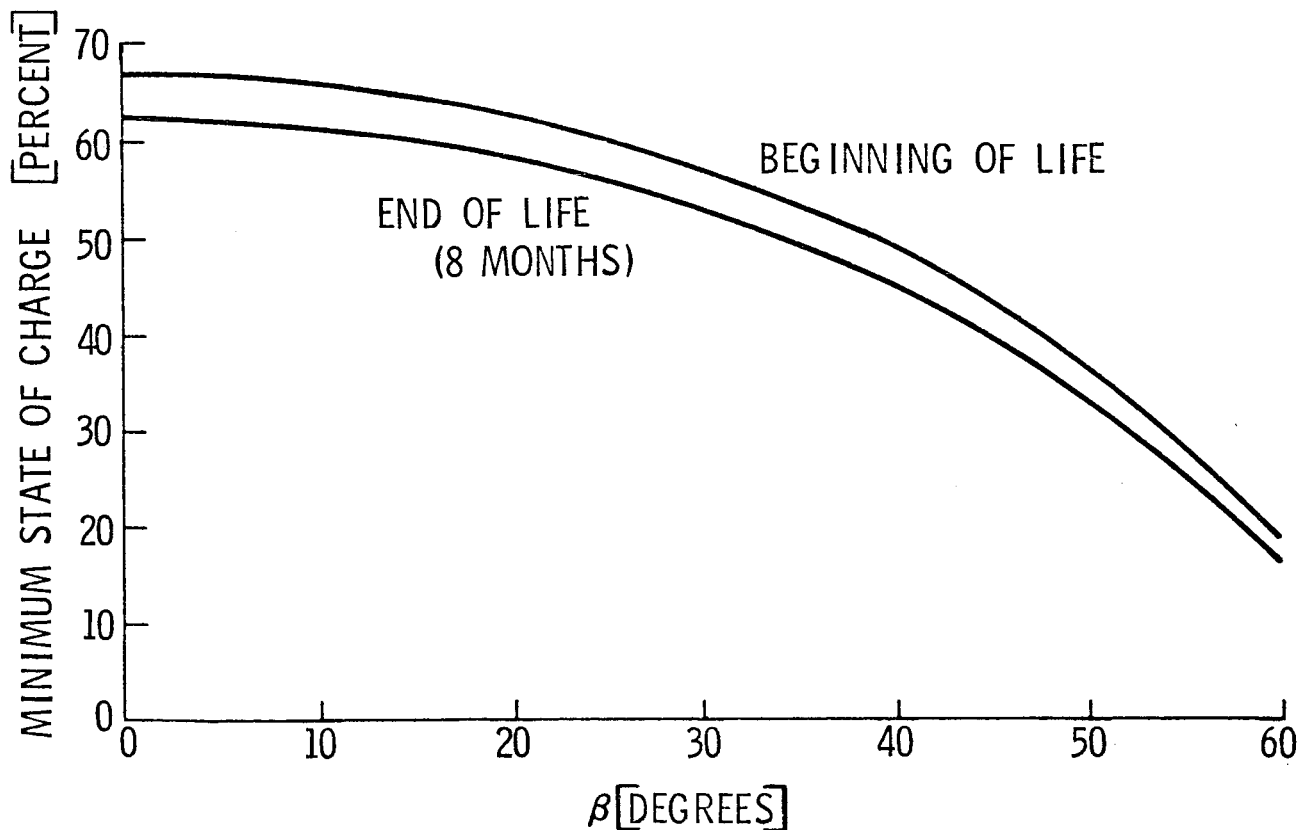

FIGURE 14 - EFFECT OF SOLAR CELL DEGRADATION

VIII.   SUMMARY AND DISCUSSION

It is impossible to firmly state the capability of
the AAP power systems to support the earth resources mission
mode in terms of number of consecutive orbits and limits on β
without knowing exactly both the minimum power requirement and
the maximum permissible battery depth of discharge. When these
numbers are known, however, one need only go to the curves
generated in this study to accurately determine the capability.
If the estimated minimum power requirements given in the last
section are close, then it is fairly safe to say that two, and
perhaps three consecutive earth resources passes are feasible
without severe restrictions on β.

In determining the permissible battery depth of
discharge, we must realize that the specified level will be
reached infrequently, and possibly never. Assuming a constant
power requirement in the earth resources mode, a specified
limit on battery DOD will be reached only when $|\beta|$ is at an
associated upper operational limit. For instance, 70% might
be specified as an acceptable DOD when $|\beta| = 60°$, which is the
experimental limit due to ground lighting restrictions. However,
we would not expect the batteries near 70% DOD very often simply
because $|\beta|$ is seldom in the neighborhood of 60°. With the
initial conditions used to generate Figure 3, $|\beta| = 60°$ will
occur only four times during the life (eight months) of the
Workshop mission, and not at all during the first 4-1/2 months.
In the first manned mission (28 days), $|\beta|$ will not get larger
than about 32°.

Observation of Figures 10 and 11 shows that a power
requirement that results in two-orbit minimum state of charge
of 30% (70% DOD) at $\beta = 60°$ does not require even a 50% discharge
at $\beta = 30°$. The same calculation for three orbits gives a dis-
charge less than 35% at $\beta = 30°$. From these considerations,
plus the fact that even if it did occur a few times it would not
be damaging, specification of a maximum permissible battery depth
of discharge of 70% at $|\beta| = 60°$ does not appear unreasonable.

If the targets for earth resources experimentation are
all in the latitude range of 30°N to 50°N (i.e. the U.S.A.),
then the plus-Z Cluster axis is not the optimum location for
the experiments. When the limits on the subsolar point, deter-
mined by target lighting constraints and the tropics, are plotted
relative to the ground track, it is found that β will be pre-
dominantly of one sign. The subsolar point will usually be
south of the sunlit ground track, which is equivalent to a
negative β. Figure 15 indicates why, under these circumstances,
an experiment location away from the plus-Z toward the minus-Y

axis by 20° to 30° would be better. Not only will the average pointing angle, λ in Equation (1), be less, but the arrays will be sunlit for more than half the orbit, assuming the experiments are continually aimed along the local vertical.
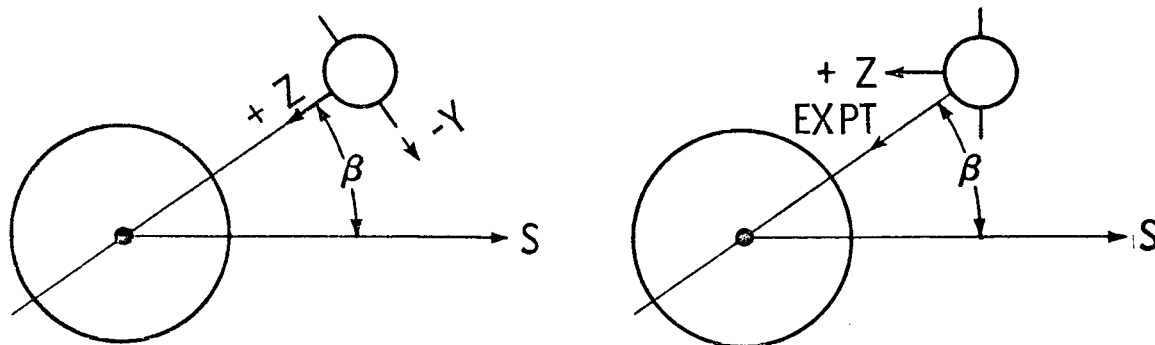
EXPT ON + Z   BETTER LOCATION

FIGURE 15 - ALTERNATE EXPERIMENT LOCATION FOR U.S.A. TARGETS

Derivation of the optimum angle for positioning the experiments vs β is the identical problem that is discussed as the Fixed Roll Case in Reference 3. One only need recognize that, in both problems, we have one spacecraft axis pointed directly down and are optimizing the position of the arrays relative to that axis with an angular degree of freedom about a line tangent to the orbit.

If targets for the earth resources experiments are equally distributed north and south of the equator, then the optimum experiment position is along the plus-Z axis.

IX.   ACKNOWLEDGEMENT

W. W. Hough

B. W. Moss

J. J. Sakolosky

WWH
1022-BWM-cf
    JJS

BELLCOMM. INC.

REFERENCES

1. Fearnsides, J. J., "A Study of Some Attitude and Control Options Compatible with the Performance of Earth-Pointing Experiments by the AAP Cluster," Technical Memorandum TM-70-1022-2, Bellcomm, Inc., February 3, 1970.

2. Apollo Applications Program - Baseline Reference Mission (Rev. A), MSC-KM-D-68-4A, NASA, Manned Spacecraft Center, Houston, Texas, October 27, 1969.

3. Hough, W. W. and Elrod, B. D., "Solar Array Performance as a Function of Orbital Parameters and Spacecraft Attitude," Journal of Engineering for Industry, Trans. ASME, Series B, Vol. 91, No. 1, February 1969, pp. 13-20.

4. Powers, J. W., "Solar Array Temperatures during the AAP-SWS Earth Pointing Experiments Mission Mode," Memorandum for File B70 01059, Bellcomm, Inc., January 28, 1970.

5. Moss, B. W., "The Effect of Quartz Coverslides on Radiant Energy Incident on Solar Cells," Memorandum for File B69 04094, Bellcomm, Inc., April 24, 1969.

6. Sakolosky, J. J., "Shading of the AAP Workshop Solar Arrays by the ATM Arrays," Technical Memorandum TM-70-1022-9, Bellcomm, Inc., March 31, 1970.

APPENDIX A

NOON-TO-NOON SATELLITE PERIOD

The period of a satellite in a circular orbit about a spherical earth is given by:

$$T_0 = 2\pi \sqrt{\frac{(R+H)^3}{\mu}}$$

A-1

where: R is the radius of the earth = 3443.93 NM

H is the altitude of the orbit

μ is the earth's gravitational constant =

$$4.68427 \cdot 10^{14} \text{ NM}^3/\text{Day}^2$$

When the earth's oblateness is considered to the order of the dominant oblateness parameter, J, there is no longer a unique period for a satellite.[A-1, A-2] Commonly used periods are the anomalistic (perigee-to-perigee) and the nodical (node-to-node). There is a third period, which we'll call the noon-to-noon period, that gives the time required for the satellite to progress from one orbital noon to the next. This is the period in which the orbit position angle used in this report, η, changes by 360°.

In reference A-3, the angle ψ is used to describe the position of orbital noon ($\eta=0$) relative to the ascending node of the orbit. The angle ψ increases with time, but not linearly, and therefore $\dot{\psi}$ is not constant. However, the average value of $\dot{\psi}$ is shown to be the difference between the rate of the earth's rotation about the sun, $\dot{\gamma}$, and the orbital regression rate, $\dot{\Omega}$.

That is:

$$\dot{\psi}_{AVG} = \dot{\gamma} - \dot{\Omega}$$

A-2

where (for circular orbits)

$$\dot{\Omega} = -\frac{JR^2 \mu^{1/2} \cos i}{(R+H)^{7/2}}$$

A-3

and

$$\dot{\gamma} = 360°/\text{solar year} = 0.01720279 \text{ rad/day}$$

with J being the first-order oblateness parameter $= 1.6234 \cdot 10^{-3}$, and i the orbital inclination.

In one noon-to-noon orbit, the angle ψ increases on the average by $\dot{\psi}_{AVG}$ times the noon-to-noon period. However, since $\dot{\psi}_{AVG}$ is already to the order J, it is sufficient to set

$$\Delta\psi_{AVG} = \dot{\psi}_{AVG} T_0 \qquad \qquad \text{A-4}$$

The time needed for the satellite to traverse through $\Delta\psi_{AVG}$ is approximately

$$\Delta T_{AVG} = \Delta\psi_{AVG}/\omega_0 \qquad \qquad \text{A-5}$$

where ω_0 is the orbital rate based on a spherical earth $= 2\pi/T_0$. Thus:

$$\Delta T_{AVG} = \dot{\psi}_{AVG} \frac{T_0^2}{\pi} \qquad \qquad \text{A-6}$$

ΔT_{AVG} is a measure of the average additional time required to reach orbital noon after passing the ascending node over the time to traverse between the same two points on the preceeding orbit. To obtain the average noon-to-noon period, the nodical period must be added.

$$T_{S_{AVG}} = T_N + \Delta T_{AVG} \qquad \qquad \text{A-7}$$

where $T_{S_{AVG}}$ is the average noon-to-noon period and T_N is the nodical period, which is given to the order J by: [A-2]

$$T_N = T_0 \left(1 - J \left(\frac{R}{R+H} \right)^2 \left(\frac{7 \cos^2 i - 1}{4} \right) \right) \qquad \qquad \text{A-8}$$

Thus the average noon-to-noon period is, to the order J

$$T_{S_{AVG}} = T_0 \left(1 - J \left(\frac{R}{R+H} \right)^2 \left[\frac{7 \cos^2 i - 1}{4} \right] \right) + \frac{\dot{\psi}_{AVG}}{\omega_0} \qquad \text{A-9}$$

The values of these parameters for a 235 NM altitude, 50°
inclination orbit are:

T_0 = .06478004 days = 1.5547209 hours

T_N = .06473644 days = 1.5536745 hours

ΔT_{AVG} = .00007073 days = .0016975 hours

$T_{S_{AVG}}$ = .06480717 days = 1.5553720 hours

REFERENCES FOR APPENDIX A

A-1   Space Technology Laboratories, Flight Performance
        Handbook for Orbital Operations, Raymond W. Wolverton,
        Editor, John Wiley and Sons, New York, 1963, pp. 2-228
        through 2-230.

A-2   NASA Sp 33 Part 1, Orbital Flight Handbook, NASA Office
        of Scientific and Technical Information, Washington,
        1963, pp. IV-21 through IV-23.

A-3   Elrod, B. D., Solar Pointing Variations in Earth Orbit
        and the Impact on Mission Design, Bellcomm TR-69-1022-1,
        February 11, 1970.